

# Kinetics of Ultraviolet and Plasma Surface Modification of Poly(dimethylsiloxane) Probed by Sum Frequency Vibrational Spectroscopy

Hongke Ye, Zhiyong Gu, and David H. Gracias<sup>\*,†</sup>

*Department of Chemical and Biomolecular Engineering and Department of Chemistry, The Johns Hopkins University, 3400 North Charles Street, Baltimore, Maryland 21218*

*Received July 26, 2005. In Final Form: October 19, 2005*

In numerous applications in microfluidics, cell growth, soft lithography, and molecular imprinting, the surface of poly(dimethylsiloxane) (PDMS) is modified from a hydrophobic methyl-terminated surface to a hydrophilic hydroxyl-terminated surface. In this study, we investigated molecular structural and orientational changes at the PDMS–air interface in response to three commonly used surface modification processes: exposure to long-wavelength ultraviolet light (UV), exposure to short-wavelength UV that generates ozone (UVO), and exposure to oxygen plasma (OP). The surfaces of two PDMS compositions (10:1 and 4:1 of base polymer/curing agent) were probed during modification, using monolayer-sensitive IR + visible sum frequency generation (SFG) vibrational spectroscopy, with two different polarization combinations. During PDMS surface modification, the peak intensities of CH<sub>3</sub> side groups and CH<sub>2</sub> cross-link groups decreased, while peak intensities of Si–OH groups increased. There was no significant change in the average orientation of the CH<sub>3</sub> groups on the PDMS surface during modification. The concentration of CH<sub>3</sub> groups on the surface decreased exponentially with time, for all three UV, UVO, and OP modification processes, with first order kinetics and time constants of approximately 160, 66, and 0.3 min, respectively. At steady state, residual CH<sub>3</sub> groups were detected at the PDMS surface for UV and UVO treatments; however, there were negligible CH<sub>3</sub> groups detected after OP modification.

## Introduction

In recent years, the rapid miniaturization of structures and devices in biology and electronics has resulted in the development of novel microfabrication strategies that feature rapid, low-cost prototyping. Several of these strategies including soft-lithography<sup>1</sup> and decal transfer lithography (DTL)<sup>2</sup> rely on the surface modification of a polymeric stamp using physical processes such as exposure to ultraviolet light (UV) and oxygen plasmas (OP). The primary polymer used in these lithographic methods is the silicon-based polymer poly(dimethylsiloxane) (PDMS) which has several attractive properties including optical transparency, chemical inertness, and elasticity.<sup>3</sup> PDMS consists of repeating (–OSi(CH<sub>3</sub>)<sub>2</sub>–) units with a hydrophobic, low-surface-energy, methyl-terminated surface. The hydrophobic nature of the surface is advantageous since it is relatively inert with low surface energy. However, in many applications in microfluidics, bioengineering, and lithography, it is necessary to render the surface of PDMS hydrophilic to improve wetting of aqueous solvents, decrease nonspecific binding of proteins and cells, and increase adhesion. It is also possible to irreversibly bond PDMS surfaces with each other or with other surfaces, immediately after oxidation, by mere contact.<sup>4</sup> This facile bonding of surface-modified PDMS is critical in pattern transfer in DTL and in the sealing of microfluidic channels.

The PDMS surface can be rendered hydrophilic using a variety of physical techniques, including exposure to UV light (in DTL) or exposure to OP (in microfluidics). In this paper, we investigated the surface modification of PDMS using the three most commonly

used physical methods (a) UV modification, exposure to long-wavelength UV light ( $\lambda = 315\text{--}400\text{ nm}$ ), (b) UVO modification, exposure to short-wavelength UV light which includes wavelengths ( $\lambda = 185/254\text{ nm}$ ), and (c) OP modification, exposure to an oxygen plasma. As opposed to long-wavelength exposure (UV), short-wavelength exposure (UVO) at 185 and 254 nm generates atomic oxygen—a very strong oxidizing agent.<sup>5,6</sup> Atomic oxygen is generated in ambient air by the combination of photochemical processes at 185 and 254 nm. The 185 nm line produces ozone from molecular oxygen by a two-step photochemical process, while the 254 nm line converts the ozone to atomic oxygen. An oxygen plasma consists of a large number of electrons and highly reactive ionic and free radical oxygen species that facilitate oxidation of surfaces.

The PDMS samples used in our experiments (Sylgard 184, the most commonly used form of PDMS) were made up of a base polymer and a curing agent. The components undergo a hydrosilylation reaction upon curing that results in cross-linking of the polymer chains.<sup>7</sup> To investigate the effect of cross-linking on the surface properties of PDMS, before and after surface modification, we investigated PDMS surfaces with different ratios (10:1 and 4:1 w/w) of base polymer to curing agent. The Sylgard 184 base polymer is composed of dimethylsiloxane oligomers with vinyl-terminated end groups, platinum catalyst, and silica filler (dimethylvinylated and trimethylated silica), while the curing agent contains a cross-linking agent (dimethylmethylhydrogen siloxane) and an inhibitor (tetramethyltetra vinyl cyclo-tetra-siloxane).<sup>8</sup> The cross-linking process occurs when vinyl and silicon hydride groups undergo a hydrosilylation reaction in the presence

<sup>\*</sup> To whom correspondence should be addressed. E-mail: dgracias@jhu.edu.

<sup>†</sup> Department of Chemistry.

(1) Xia, Y. N.; Whitesides, G. M. *Annu. Rev. Mater. Sci.* **1998**, *28*, 153–184.

(2) Childs, W. R.; Nuzzo, R. G. *J. Am. Chem. Soc.* **2002**, *124*, 13583–13596.

(3) Sia, S. K.; Whitesides, G. M. *Electrophoresis* **2003**, *24*, 3563–3576.

(4) McDonald, J. C.; Whitesides, G. M. *Acc. Chem. Res.* **2002**, *35*, 491–499.

(5) Vig, J. R.; LeBus, J. W. U.S. Patent 4,028,135, 1977.

(6) Muisener, R. J.; Koberstein, J. T. *Polym. Mater. Sci. Eng.* **1997**, *77*, 653.

(7) Simpson, T.; Jeynes, C.; Parbhoo, B.; Keddie, J. L. *J. Polym. Sci. A* **2004**, *42*, 1421–1431.

(8) Lee, J. N.; Jiang, X.; Ryan, D.; Whitesides, G. M. *Langmuir* **2004**, *20*, 11684–11691.

of the catalyst to form a Si–C bond, thereby facilitating (–CH<sub>2</sub>–CH<sub>2</sub>–) linkages between PDMS chains (Figure 1).<sup>9,10</sup> Even though the 10:1 composition of PDMS is widely used, a fraction of uncured oligomers as high as 5% of the total weight of the polymer has been reported.<sup>11</sup> Since 4:1 PDMS has a higher fraction of curing agent, the (–CH<sub>2</sub>–CH<sub>2</sub>–) cross-linking is expected to be higher as compared to the 10:1 sample.

Previous studies of the modification of the PDMS surface using FT-IR spectroscopy,<sup>12,13</sup> contact-angle goniometry,<sup>14,15</sup> chemical force microscopy,<sup>16</sup> secondary ion mass spectrometry (SIMS),<sup>17</sup> near-edge X-ray absorption fine structure (NEXAFS),<sup>18</sup> and X-ray photoelectron spectroscopy (XPS)<sup>19–21</sup> have provided some information regarding the mechanism of oxidation of the PDMS surface, but information regarding the kinetics of surface molecular changes is lacking. Additionally, it is difficult to detect surface-specific molecular concentration and orientation changes at a polymer interface using FT-IR due to limited surface sensitivity. While contact-angle goniometry does provide valuable information about the surface energy, it is not possible to get a molecular-level understanding. Although SIMS, NEXAFS, and XPS are extremely surface sensitive, they require vacuum operation, and the studies done using these spectroscopies involved a time delay between modification of the polymer and the spectroscopic measurement. Hence, using these spectroscopies, it has not been possible to study the PDMS surface in-situ during modification, or in an ambient environment of air where PDMS is most commonly used. In this paper, we used surface-specific IR + visible sum frequency generation (SFG) spectroscopy<sup>22</sup> to probe the structural changes on the PDMS surface. SFG measurements of UV and UVO modification were recorded in situ as a function of time; measurements of OP modification were done in air immediately after irradiation. By using different optical polarization combinations,<sup>23</sup> we were also able to monitor molecular orientation at the surface of PDMS during UV, UVO, and OP modification.

SFG<sup>24</sup> is a nonlinear surface-specific spectroscopic technique that allows nondestructive analysis of the surface of a sample in air. It has been convincingly demonstrated, both on the basis of theoretical and experimental studies, that SFG spectroscopy has monolayer sensitivity for polymers<sup>25</sup> that possess bulk inversion symmetry; the surface sensitivity is a result of the fact that this second-order nonlinear optical process vanishes under

centrosymmetry. SFG has been used to study the surface oxidation and UV-induced modification of polymers including polystyrene,<sup>26,27</sup> polyimide,<sup>28</sup> and poly(ethylene terephthalate)<sup>29</sup> with high surface sensitivity. The SFG spectroscopy involved overlapping a visible beam ( $\omega_{\text{VIS}}$ ) and a tunable IR ( $\omega_{\text{IR}}$ ) beam at the surface of the PDMS. The surface vibrational spectrum was obtained by tuning the IR beam over the relevant resonant vibrational modes and measuring the intensity of the reflected sum frequency (SF) ( $\omega_{\text{SF}} = \omega_{\text{VIS}} + \omega_{\text{IR}}$ ) beam as a function of IR frequency.

This paper is the first SFG study of the modification of PDMS using either UV, UVO, or OP modification. The measurements were conducted under relevant ambient conditions and are surface sensitive. We were able to monitor concentrations relative to orientations of the surface groups in-situ, which has allowed us to develop a quantitative kinetic model for the modification processes.

## Experimental Section

**Materials Used.** Two compositions of PDMS (Dow Corning Sylgard 184, two-component kit) were prepared by vigorously mixing 10:1 and 4:1 (w/w) ratios of the base polymer to curing agent. After the mixture was degassed using vacuum, the polymer was spun on quartz substrates (1 in. diameter, 1/8 in. thick, Esco Products) at 5000 rpm for 30 s and subsequently cured at 65 °C for 4 h. The spin-coated films had a thickness of  $\sim 1.8 \mu\text{m}$  as measured by profilometry. We also cast thick films (1 cm) of PDMS by pouring the mixture of base polymer and curing agent into a Petri dish and subsequently curing it.

**Surface Modification.** Three different surface-modification strategies were used. (a) UV modification by exposure to a long wavelength ( $\lambda = 315\text{--}400 \text{ nm}$ , peaked at 365 nm), B-100A mercury lamp (UVP, Inc., www.uvp.com). The intensity at the sample was measured using a UV power meter and was  $\sim 4 \text{ mW/cm}^2$  at  $\lambda = 365 \text{ nm}$ . (b) UVO modification by exposure to a low-pressure, short wavelength mercury PEN-RAY lamp (UVP, Inc., www.uvp.com) with line emissions at 185 and 254 nm. The intensity at the sample was comparable to the UV exposure,  $\sim 4 \text{ mW/cm}^2$  at  $\lambda = 254 \text{ nm}$ . (c) OP modification by exposure to an 18 W radio frequency Harrick Scientific plasma source (PDC-32G, http://www.harricksci.com/plasma.cfm) in a background pressure of 200 mTorr.

**SFG.** A tunable IR and visible laser beam were spatially and temporally overlapped on the PDMS surface at incident angles of 55° and 60°, respectively, relative to the surface normal. We used a solid-state mode-locked Nd:YAG laser (1064 nm, 31 ps pulse, 10 Hz repetition rate, EKSPLA, Inc., www.ekspla.com) to generate both the visible and the tunable IR beam. The fundamental laser output with a frequency at  $\lambda = 1064 \text{ nm}$  was doubled using a type I potassium dideuterium phosphate crystal to generate the visible  $\lambda = 532 \text{ nm}$  beam. The tunable IR beam was generated using a combination of optical parametric generation (OPG)/optical parametric amplification (OPA) based on a lithium triborate crystal and difference frequency generation (DFG) based on a silver gallium sulfide (AgGaS<sub>2</sub>) crystal. The frequency of the IR beam was tuned between 2800 and 3500  $\text{cm}^{-1}$ ; the output energy was  $\sim 200 \mu\text{J}$  in this frequency region. The SFG signal was measured using a monochromator in reflection geometry.

**Spectral Fitting.** SFG spectra were obtained with two different polarization combinations ssp (s-polarized SF output, s-polarized visible input, and p-polarized infrared input) and sps. Using the two polarizations it was possible to get information of relative orientation of chromophores at the surface. The SF beam consists of a nonresonant term and a resonant term, so that the measured reflected

(9) Hammouch, S. O.; Beinert, G. J.; Zilliox, J. G.; Herz, J. E. *Polymer* **1995**, 36, 421–426.

(10) Fu, P. F.; Glover, S.; King, R. K.; Lee, C. L.; Pretzer, M. R.; Tomalia, M. K. *Polym. Prepr.* **2003**, 44, 1014–1015.

(11) Lee, J. N.; Park, C.; Whitesides, G. M. *Anal. Chem.* **2003**, 75, 6544–6554.

(12) Berdichevsky, Y.; Khandurina, J.; Guttman, A.; Lo, Y. H. *Sens. Actuators, B* **2004**, 97, 402–408.

(13) Graubner, V. M.; Jordan, R.; Nuyken, O.; Schnyder, B.; Lippert, T.; Kotz, R.; Wokaun, A. *Macromolecules* **2004**, 37, 5936–5943.

(14) Chaudhury, M. K.; Whitesides, G. M. *Langmuir* **1991**, 7, 1013–1025.

(15) Chen, L.; Ren, J. C.; Bi, R.; Chen, D. *Electrophoresis* **2004**, 25, 914–921.

(16) Hillborg, H.; Tomczak, N.; Olah, A.; Schonherr, H.; Vancso, G. J. *Langmuir* **2004**, 20, 785–794.

(17) Childs, W. R.; Michael, M. J.; Lee, K. J.; Nuzzo, R. G. *Langmuir* **2005**, 21, 10096–10105.

(18) Efimenko, K.; Wallace, W. E.; Genzer, J. J. *Colloid Interface Sci.* **2002**, 254, 306–315.

(19) Ouyang, M.; Yuan, C.; Muisener, R. J.; Boulares, A.; Koberstein, J. T. *Chem. Mater.* **2000**, 12, 1591–1596.

(20) Schnyder, B.; Lippert, T.; Kotz, R.; Wokaun, A.; Graubner, V. M.; Nuyken, O. *Surf. Sci.* **2003**, 532, 1067–1071.

(21) Graubner, V. M.; Jordan, R.; Nuyken, O.; Schnyder, B.; Lippert, T.; Kotz, R.; Wokaun, A. *Macromolecules* **2004**, 37, 5936–5943.

(22) Zhu, X. D.; Suhr, H.; Shen, Y. R. *Phys. Rev. B* **1987**, 35, 3047–3050.

(23) Guyotssonnet, P.; Hunt, J. H.; Shen, Y. R. *Phys. Rev. Lett.* **1987**, 59, 1597–1600.

(24) Shen, Y. R. *Nature* **1989**, 337, 519–525.

(25) Gracias, D. H.; Chen, Z.; Shen, Y. R.; Somorjai, G. A. *Acc. Chem. Res.* **1999**, 32, 930–940.

(26) Zhang, D.; Dougal, S. M.; Yeganeh, M. S. *Langmuir* **2000**, 16, 4528–4532.

(27) Li, J.; Oh, K.; Yu, H. *Chin. J. Polym. Sci.* **2005**, 23, 187–196.

(28) Oh-e, M.; Kim, D.; Shen, Y. R. *J. Chem. Phys.* **2001**, 115, 5582–5588.

(29) Miyamae, T.; Yamada, Y.; Uyama, H.; Nozoye, H. *Appl. Surf. Sci.* **2001**, 180, 126–137.

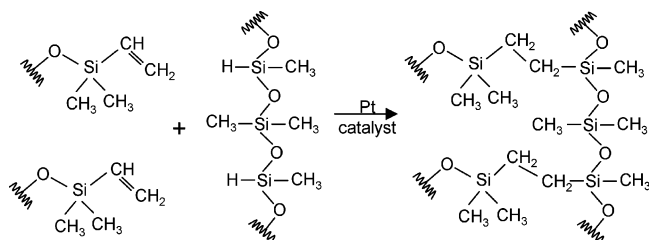


**Figure 1.** Schematic diagram of the PDMS curing process. The base polymer (containing dimethylsiloxane oligomers with vinyl-terminated end groups) reacts with the curing agent (containing dimethylmethylhydrogen siloxane) in the presence of a platinum catalyst to form cross-links between oligomers.

intensity from the sample, for the ssp and sps polarization combination, is given by,

$$I_{\text{ssp}}^{\text{SF}} \propto |\chi_{\text{yyz}}^{(2)}|^2 \text{ and } I_{\text{sps}}^{\text{SF}} \propto |\chi_{\text{yzy}}^{(2)}|^2$$

where

$$\chi^{(2)} = \chi_{\text{NR}}^{(2)} + \chi_{\text{R}}^{(2)} = \chi_{\text{NR}}^{(2)} + \sum_q \frac{A_q}{\omega_{\text{IR}} - \omega_q + i\Gamma_q} \quad (1)$$

$\chi_{\text{NR}}^{(2)}$  and  $\chi_{\text{R}}^{(2)}$  are the second-order nonresonant and resonant nonlinear optical susceptibilities. The frequency of the incident IR beam, the strength, damping constant, and resonance frequency of the  $q$ th vibrational mode in a given polarization combination are denoted by  $\omega_{\text{IR}}$ ,  $A_q$ ,  $\Gamma_q$ , and  $\omega_q$ , respectively. All SFG spectra were normalized by the intensities of the IR and visible beams to compensate for the effects of intensity fluctuations and absorption. The SFG spectra presented in the paper include both the raw measured data points and a solid line representing a fit to eq 1 to the data. By measuring the SFG spectra with ssp and sps polarization combinations, and fitting the data to the eq 1, information about  $\chi_{\text{R,yyz}}^{(2)}$  and  $\chi_{\text{R,yzy}}^{(2)}$  were obtained that allowed us to get molecular orientational information.<sup>30,31</sup>

## Results and Discussion

The SFG spectra obtained on spin-coated PDMS films using ssp and sps polarizations for 10:1 PDMS and 4:1 PDMS are shown in Figure 2. The circles represent the raw data, and the solid line represents the fit to eq 1. The ssp spectra were dominated by the symmetric stretch ( $\text{CH}_3\text{-ss}$ ) of the methyl side groups at  $2910\text{ cm}^{-1}$ , while the sps spectra were dominated by the antisymmetric stretch ( $\text{CH}_3\text{-as}$ ) at  $2960\text{ cm}^{-1}$ . These results are consistent and assigned on the basis of published SFG spectra for PDMS<sup>32</sup> and PDMS FTIR spectra.<sup>12,13,18</sup> The strong polarization dependence of the symmetric and antisymmetric peaks indicates that the methyl groups have their symmetric axes more or less along the surface normal.<sup>33,34</sup> Additional peaks observed in the SFG spectra of 4:1 PDMS at  $2850\text{ cm}^{-1}$  (in ssp) and  $2915\text{ cm}^{-1}$  (in sps) were assigned<sup>35–37</sup> to the symmetric ( $\text{CH}_2\text{-ss}$ ) and the antisymmetric ( $\text{CH}_2\text{-as}$ ) stretches expected in  $(-\text{Si}-\text{CH}_2-\text{CH}_2-$

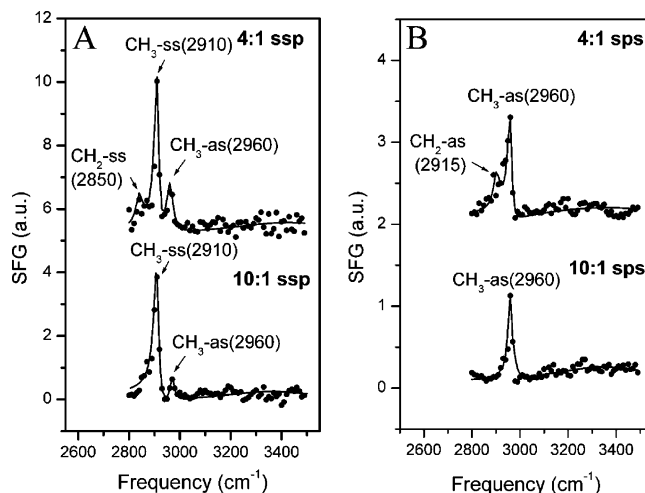


**Figure 2.** SFG spectra of 10:1 and 4:1 PDMS taken in air with the polarization combinations (A) ssp (for s-polarized SF output, s-polarized visible input, and p-polarized infrared output) and (B) sps. The circles are the raw data, and the solid line is a fit to eq 1.

$\text{Si-}$ ) linkages. The presence of  $\text{CH}_2$  peaks on 4:1 PDMS and their absence on 10:1 PDMS in both ssp and sps spectra leads us to conclude that there is an increase in  $(-\text{CH}_2-\text{CH}_2-)$  linkages on the 4:1 PDMS surface as compared to the 10:1 PDMS surface. To confirm that the SFG signal being monitored on spin-coated films was from the air–PDMS interface and not the PDMS–substrate interface, we also obtained spectra on very thick (1 cm) PDMS films. For thick PDMS films, light from the PDMS–substrate interface was blocked from entering the PMT using an aperture. The SFG spectra of thick films were similar to thin spin-coated PDMS films, confirming that the SFG signal being monitored on spin-coated PDMS films was from the PDMS–air interface. Although the spectra in both thin and thick films were similar to each other, the signal-to-noise ratio was higher for spin-coated PDMS films as their surfaces were smoother resulting in lower scattering. Hence, all the spectra reported in the paper were obtained with thin ( $\sim 1.8\text{ }\mu\text{m}$ ) spin-coated PDMS films. It should be noted that numerous SFG studies probing polymer interfaces utilize spin coated films for similar reasons. In a previous study by Wang et al., the authors obtained similar SFG spectra for thin and thick PMMA films, concluding that the surface being probed was the air–polymer interface. They argue that the IR beam intensity is depleted on passing through the polymer bulk to the polymer–substrate interface (due to absorption).<sup>38</sup>

The average value of the ratio  $|\chi_{\text{yyz,as}}|/|\chi_{\text{yzy,as}}|$  for methyl groups on the surface of 10:1 and 4:1 PDMS was 0.76 and 0.89, while the ratio of  $|\chi_{\text{yyz,as}}|/|\chi_{\text{yzy,s}}|$  on the surface of 10:1 and 4:1 PDMS was 0.42 and 0.58. These values of  $\chi_{\text{yyz,as}}$ ,  $\chi_{\text{yzy,as}}$ , and  $\chi_{\text{yzy,s}}$  were obtained by measuring SFG spectra on 10:1 and 4:1 PDMS surfaces using ssp and sps polarization combinations. We repeated each experiment on four different PDMS samples and computed the ratios for each sample. Taking into account the effect of the baseline noise level observed on the SFG spectra, the error of the mean value calculated for each ratio (from four samples) was in the range of 0.02–0.04.

A detailed analysis for determining the average orientation angle ( $\theta$ ) of the methyl group vs the surface normal and the angle distribution parameter ( $\sigma$ ) based on the two ratios  $|\chi_{\text{yyz,as}}|/|\chi_{\text{yzy,as}}|$  and  $|\chi_{\text{yyz,as}}|/|\chi_{\text{yzy,s}}|$  has been outlined in prior publications<sup>30–32</sup> by treating the methyl side groups on PDMS with  $C_{3v}$  symmetry.

(30) Hirose, C.; Yamamoto, H.; Akamatsu, N.; Domen, K. *J. Phys. Chem.* **1993**, *97*, 10064–10069.

(31) Hirose, C.; Akamatsu, N.; Domen, K. *J. Chem. Phys.* **1992**, *96*, 997–1004.

(32) Chen, C. Y.; Wang, J.; Chen, Z. *Langmuir* **2004**, *20*, 10186–10193.

(33) Zhang, D.; Ward, R. S.; Shen, Y. R.; Somorjai, G. A. *J. Phys. Chem. B* **1997**, *101*, 9060–9064.

(34) Zhang, D.; Gracias, D. H.; Ward, R.; Gauckler, M.; Tian, Y.; Shen, Y. R.; Somorjai, G. A. *J. Phys. Chem. B* **1998**, *102*, 6225–6230.

(35) Zhang, D.; Shen, Y. R.; Somorjai, G. A. *Chem. Phys. Lett.* **1997**, *281*, 394–400.

(36) Lu, R.; Gan, W.; Wu, B.; Zhang, Z.; Guo, Y.; Wang, H.-F. *J. Phys. Chem.* **2005**, *109*, 14118–14129.

(37) Zhuang, X.; Miranda, P. B.; Kim, D.; Shen, Y. R. *Phys. Rev. B* **1999**, *59*, 12632–12640.

(38) Wang, J.; Chen, C.; Buck, S. M.; Chen, Z. *J. Phys. Chem.* **2001**, *105*, 12118–12125.



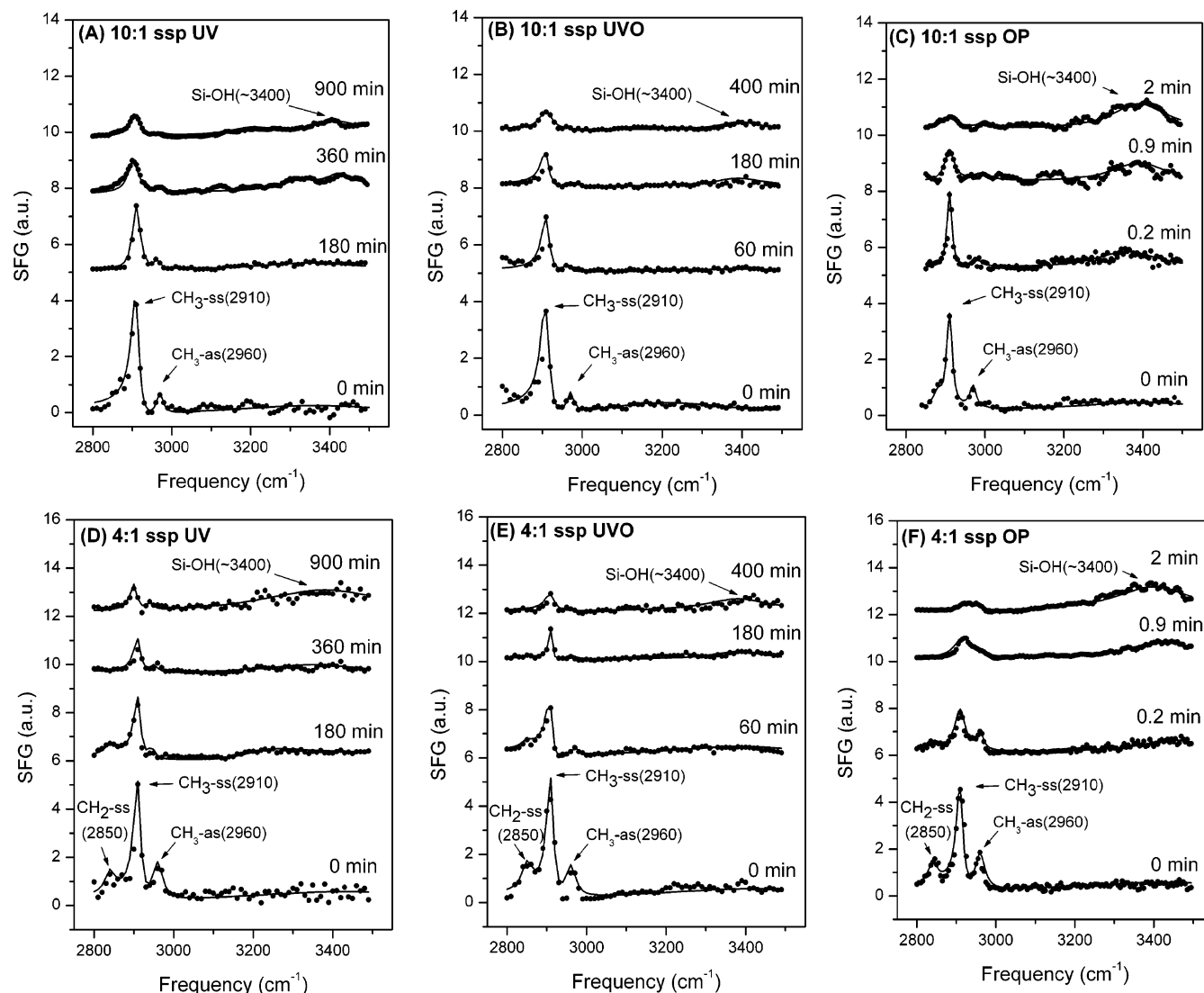


**Figure 3.** SFG ssp spectra of (A)–(C) 10:1 PDMS on exposure to (A) UV, (B) UVO, and (C) OP. (D)–(F) 4:1 PDMS on exposure to (D) UV, (E) UVO, and (F) OP. The circles are the raw data, and the solid line is a fit to eq 1 for the polarization combination used. We observe a trend for all three modification processes: there is a pronounced decrease in the  $\text{CH}_x$  peak intensities and an increase in the intensity of a broad peak centered at approximately  $3400\text{ cm}^{-1}$  that was assigned to Si–OH groups.

We utilized a similar analysis (based on our peak assignments and ratios), assuming a delta function angle distribution, to determine a tilt angle of  $\sim 40^\circ$  with respect to the surface normal for the 10:1 sample and a larger angle of  $\sim 45^\circ$  for the 4:1 sample. One reason for this orientation difference of the  $\text{CH}_3$  groups for 10:1 and 4:1 may be due to increased density (more cross-linking) expected on the 4:1 surface as a result of an increased fraction of curing agent and as observed by the presence of  $\text{CH}_2$  groups in the SFG spectra. An increase in the average orientation angle of  $\text{CH}_3$  side groups (with respect to the surface normal) with increased density has been observed before in SFG studies of polypropylene.<sup>35,39</sup> In addition to increased ( $-\text{CH}_2-\text{CH}_2-$ ) linkages between polymer chains, since the 4:1 sample contains a higher fraction of inhibitor, ( $-\text{CH}_2-\text{CH}_2-$ ) linkages of the polymer chains to the inhibitor molecules may also affect the  $\text{CH}_2$  peak intensity and  $\text{CH}_3$  group average orientation.

In summary, using SFG we have observed two main differences between 4:1 PDMS and 10:1 PDMS;  $\text{CH}_2$  groups can be detected on the surface of 4:1 PDMS and the  $\text{CH}_3$  groups on average are closer to the surface in 4:1 PDMS. These two differences may

provide a molecular-level explanation for the increase in water contact angle measured (greater hydrophobicity) by Lee et al.<sup>8</sup> for PDMS samples containing an increased fraction of curing agent.

SFG ssp spectra for 10:1 and 4:1 PDMS that were modified by UV, UVO, and OP were measured at different exposure times (Figure 3). A universal trend observed in the spectra was a decrease in the intensity of both  $\text{CH}_3$  and  $\text{CH}_2$  modes at 2850, 2910, and  $2960\text{ cm}^{-1}$  and an increase in intensity of a broad peak centered at  $\sim 3400\text{ cm}^{-1}$ . This peak at  $3400\text{ cm}^{-1}$  has been observed before in FT-IR<sup>12,13</sup> studies on modified PDMS and was assigned to O–H vibrational modes in Si–OH. Hence, on exposure to UV, UVO, and OP, the PDMS surface is modified from a  $\text{CH}_x$ -covered surface to an OH-covered surface. For both UV and UVO modification,  $\text{CH}_3$  groups were detected even at long exposure times, while for OP modification, a negligible (i.e., within the present signal-to-noise detection capability, estimated at about 5% of the initial concentration) fraction of  $\text{CH}_3$  groups were observed on the surface after exposure for only 2 min.

In addition to ssp spectra, we also measured sps spectra for 10:1 and 4:1 PDMS during modification by UV, UVO, and OP. The sps spectra showed a similar trend of a decrease in the

(39) Gracias, D. H.; Zhang, D.; Lianos, L.; Ibach, W.; Shen, Y. R.; Somorjai, G. A. *Chem. Phys.* **1999**, *245*, 277–284.

intensity of the  $\text{CH}_x$  vibrational modes and an increase in Si–OH peak intensity. Using both the ssp and sps spectra, we were able to calculate molecular orientational changes of the  $\text{CH}_3$  side groups of the polymer. Within experimental noise, there was no discernible change in the average orientation of  $\text{CH}_3$  as the values of  $|(\chi_{yyz,as})/(\chi_{zyy,as})|$  and  $|(\chi_{yyz,as})/(\chi_{yyz,s})|$  remained roughly constant during the surface modification. This observation is consistent with a local chain scission and oxidation mechanism with relatively no long-range average orientational perturbation of the chains.

We measured in-situ kinetics of UV and UVO modification of 10:1 PDMS by monitoring SFG intensity for the symmetric ( $\text{CH}_3$ -ss) stretch at  $2910\text{ cm}^{-1}$  using ssp polarization and the antisymmetric ( $\text{CH}_3$ -as) stretch at  $2960\text{ cm}^{-1}$  using sps polarization. We chose to monitor these two  $\text{CH}_3$  peaks since they were well resolved, had high signal-to-noise ratios, and their peak position remained unchanged during the modification process. The intensity of the peaks was measured over a period of several hours. The normalized value of  $A/T$  (derived by fitting eqs 1 to the data) for the ssp peak at  $2910\text{ cm}^{-1}$  and the sps peak at  $2960\text{ cm}^{-1}$  are plotted in Figure 4. The normalized value of  $A/T$  at these frequencies that is proportional to the concentration of  $\text{CH}_3$  groups at the surface decreases exponentially with time for all three modification processes. The normalized value of  $A/T$  for the symmetric ( $\text{CH}_3$ -ss) stretch at  $2910\text{ cm}^{-1}$  in ssp polarization and the antisymmetric ( $\text{CH}_3$ -as) stretch at  $2960\text{ cm}^{-1}$  in sps polarization fell at approximately the same rate, which confirms our earlier observation that there is practically no change in the orientation of the  $\text{CH}_3$  groups during surface modification. We also performed the same experiment using 4:1 PDMS and observed similar results. At steady state, we observed the presence of  $\text{CH}_3$  groups on both UV- and UVO-modified PDMS surfaces. This is in agreement with published XPS results,<sup>19–21</sup> obtained on the surface of PDMS, that shows the presence of carbon even after long exposures of UV and UVO. However, after OP modification, the concentration of  $\text{CH}_3$  groups at the surface was negligible.

Our data suggest first-order reaction kinetics for the change in concentration of the  $\text{CH}_3$  group on the surface as detailed below. Denoting  $k_1$  as the rate of removal of  $\text{CH}_3$  groups from the surface and  $k_{-1}$  as the rate of regeneration of  $\text{CH}_3$  groups at the surface, the first-order reaction rate for the change of  $\text{CH}_3$  groups at the surface can be written as

$$\frac{dc_t}{dt} = -k_1 c_t + k_{-1}(c_0 - c_t) \quad (2)$$

where  $c_t$  and  $c_0$  are the concentrations of the  $\text{CH}_3$  groups at time  $t$  and time zero (the initial concentration).

Applying steady-state conditions,  $k_1 c_s = k_{-1}(c_0 - c_s)$ , where  $c_s$  is the concentration of the  $\text{CH}_3$  groups at steady state, and integrating with limits of  $t = 0 \Rightarrow c_t = c_0$  yields an equation of the form

$$y = a + (1 - a) \exp(-t/\tau) \quad (3)$$

with  $y = (c_t/c_0)$ ,  $a = (c_s/c_0)$ , and  $\tau = (c_0 - c_s)/k_1 c_0$ . We get an excellent fit of eq 3 to the SFG data plotted in Figure 4. On the basis of the equation fitting, the normalized steady-state concentration ( $c_s/c_0$ ) of  $\text{CH}_3$  groups at the surface for ssp polarization are 0.33, 0.29, and 0.02; the decay time constants are 160, 66, and 0.3 min for UV, UVO, and OP modification, respectively. Since the signal-to-noise ratio was higher for sps spectra, less scatter was observed for sps spectra; nevertheless, similar values and trends were observed for ssp polarization.

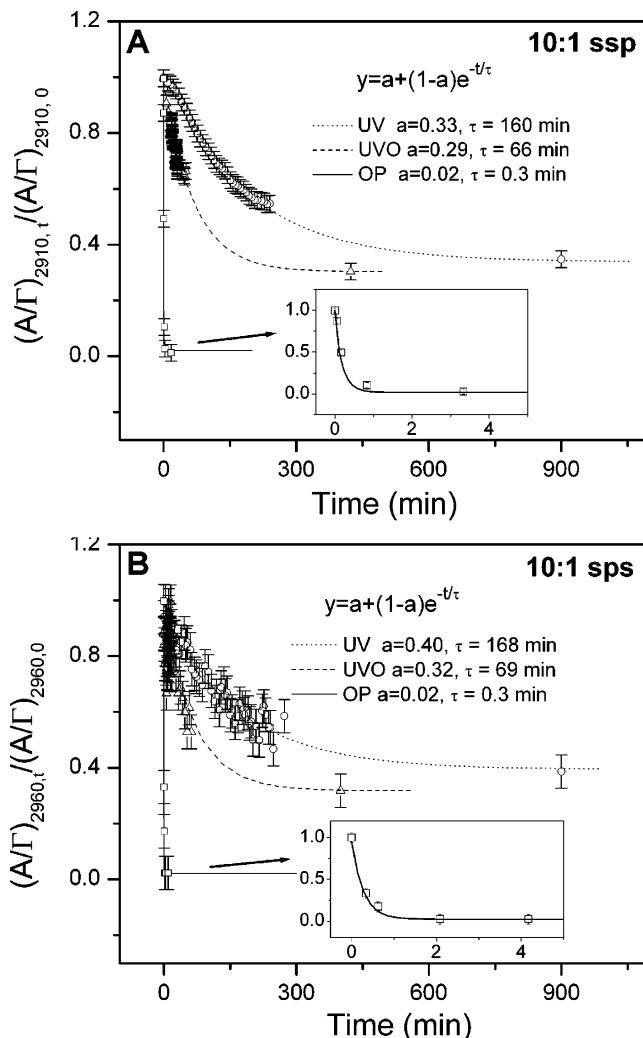


**Figure 4.** Plots of normalized  $(A/T)$ , from eq 1, of the (A) symmetric ( $\text{CH}_3$ -ss) stretch at  $2910\text{ cm}^{-1}$  and (B) antisymmetric ( $\text{CH}_3$ -as) stretch at  $2960\text{ cm}^{-1}$  monitored as a function of time for 10:1 PDMS using ssp and sps polarization combinations during UV, UVO, and OP modification. The circles, squares, and triangles were derived by fitting spectra to eq 1 for the polarization combination used. The dashed and solid lines in the figure are a fit of eq 3 to the data. The normalized value of  $(A/T)$  that is proportional to the concentration of  $\text{CH}_3$  groups on the surface of PDMS decreases exponentially for UV, UVO, and OP (also see zoomed inset for OP) modification with a first-order reaction rate.

These results show that UV modification has the least effect on the PDMS surface, with a large fraction of residual  $\text{CH}_3$  groups. It has been hypothesized that UV radiation is primarily responsible for chain scission and the generation of free radicals, with limited oxidation.<sup>18</sup> UVO modification is much faster due to the presence of atomic oxygen, but a fraction of the methyl groups are still present on the surface at steady state, this fraction being smaller than that observed in UV irradiation. In OP modification, the surface of PDMS is very rapidly transformed into a hydroxyl-terminated surface, with negligible residual  $\text{CH}_3$  groups. We explain this by noting that OP plasma is a very powerful oxidizing source, with the presence of highly reactive ionic and free radical species; hence, efficient oxidation accompanies chain scission and the surface is rapidly modified into a hydroxylated silica-like surface. In both UV and UVO modification, we have observed kinetics that point toward a mechanism consistent with the removal, as well as regeneration, of  $\text{CH}_3$  groups at the PDMS surface. In the future, it will be interesting to use SFG spectroscopy on isotope-labeled PDMS samples to elucidate detailed mecha-

nistic pathways since it is possible that multiple multistep chemical reactions may be occurring at the same time. At the present time, we can only speculate on possible mechanisms for regeneration of  $\text{CH}_3$  groups on the basis of our results and published literature.<sup>15–20,40</sup> It has been suggested that the attack of radicals containing  $\text{CH}_3$  groups, the reorientation of PDMS molecules at the surface during modification, and migration of PDMS molecules (or oligomers) from the bulk during modification could all contribute to  $\text{CH}_3$  group regeneration. In our SFG experiments, we observe no significant change in reorientation of PDMS molecules at the surface during modification.

### Conclusion

In conclusion, we have monitored the surface modification of PDMS by UV, UVO, and OP using SFG. We observed that  $\text{CH}_3$  and  $\text{CH}_2$  groups on the surface decreased during all three modification processes and  $\text{Si}-\text{OH}$  groups were detected. There was no discernible change in the average orientation of the side

groups of the polymer during the modification process. The change of  $\text{CH}_3$  groups at the surface follows first-order kinetics and is fastest for  $\text{OP} > \text{UVO} > \text{UV}$ . At steady state, OP modification transforms the PDMS surface from a  $\text{CH}_3$ -terminated surface to one that has negligible  $\text{CH}_3$  groups, whereas UV and UVO modification leave a fraction of  $\text{CH}_3$  groups on the surface. On the basis of our results, we believe that it is possible to tailor the fraction of hydroxyl groups at the surface precisely using UV, UVO, or OP modification. With increasing oxidation, it has been observed<sup>14,15,18</sup> that the PDMS surface has a much lower water contact angle and is significantly more mechanically rigid ( $\text{SiO}_2$ -like) as compared to the hydrophobic, native PDMS surface. Tailoring the surface properties is critical in many applications of PDMS in microfluidics, cell engineering, and lithography.

**Acknowledgment.** We acknowledge funds received from a National Science Foundation (NSF- MRI- CHE-0421010) equipment grant that was used to acquire and set up the SFG laser spectroscopy system.

LA052030R

---

(40) West, J. K. *J. Biomed. Mater. Res.* **1997**, *35*, 505–511.